Unified microscopic theory of hadron and light fragment inclusive production in relativistic heavy ion collisions

Rudi Malfliet
Kernfysisch Versneller Instituut, 9747 AA Groningen, The Netherlands

Bernd Schürmann
Physik-Department, Technische Universität München, D-8046 Garching, Federal Republic of Germany

(Received 24 August 1984)

With the relativistic Boltzmann equation as a basis, we present a physically transparent theoretical approach to hadron and light fragment production in high energy nucleus-nucleus collisions. By use of multiple scattering expansion techniques and methods of transport theory, in combination with considerations from statistical thermodynamics, we arrive at a simple and practical model. Its flexibility and usefulness is demonstrated by a comparison with a variety of experimental data in the bombarding energy range of 400 MeV/nucleon to 2.1 GeV/nucleon.

I. INTRODUCTION

Heavy ion collisions in the energy range from 250 MeV to 2 GeV per nucleon have been studied extensively, both experimentally and theoretically.[1] This has led to a reasonably global insight into the reaction dynamics, especially with respect to inclusive observables ($A_1+A_2 \rightarrow M+X$ where the particle M is detected and the remainder, X, is summed over). Among all the models which have been proposed to explain the experimental data we mention explicitly the intranuclear cascade (INC) model.[2] Here, the collision of two nuclei is assumed to proceed through a superposition of individual particle-particle interactions resulting in a complicated cascade. The INC model is then a simulation of the classical microscopic behavior of colliding nucleons and is closely related to the Boltzmann equation.[3] This nonequilibrium kinetic equation is valid for dilute systems and should be a reasonable starting point to describe inclusive data since these are dominated by peripheral collisions where high densities are not so easily reached. More exclusive data like the recently measured high-multiplicity events[4,5] reflect much more the high density regimes in a nucleus-nucleus collision and so far INC models do not reproduce the observed features. Here, new approaches are needed[6] which may give rise to new and unexpected physics.

Inclusive observables, and we will restrict ourselves to these, are dominated by phase space. Still, a number of nonequilibrium features show up in the data which are related to specific nucleon-nucleon dynamics and the transparency of light nuclei for each other. Also, the production of composites (deuterons, ^{3}He,...) and mesons (π,K,...) in these reactions[7] gives rise to some interesting observations and should be treated at the same level as the nucleonic degrees of freedom. One might then be able to determine for example why the pion spectra have a different shape compared to the proton spectra. In order to obtain a satisfactory understanding of these and other aspects we need a simple and transparent approach. At the same time it should offer a reliable description of inclusive data without the complexity of a Monte-Carlo simulation as in the INC models.

In Sec. II we describe such an approach which is based on the Boltzmann equation. Through a multiple collision expansion, the eikonal approximation, and the use of transport theory ingredients, one reaches in a straightforward manner the objective, an attractive and practical model. When combined with the Hagedorn statistical thermodynamics prescription of strong interactions,[8,9] it provides also for the possibility to calculate the production of composites and some features of pion production. For the latter it is moreover necessary to include explicitly the isobar degree of freedom. In Sec. III we collect some of our results. We compare the performance of our model with a number of results obtained by INC models and the corresponding experimental data. Furthermore, we specifically address ourselves to the questions raised before and we point out a number of nonequilibrium features which play an important role in these reactions. Finally, in Sec. IV we present our conclusions. The emphasis of the paper lies in the detailed derivation of the model itself, which contains only one free parameter which is the nuclear freeze-out volume. While some of the results have already been used intuitively, it becomes now clear which assumptions are involved (and whether they are reasonable) in order to deduce it from the Boltzmann equation. This equation, we believe, is the appropriate starting point to describe nonequilibrium phenomena as they occur in high-energy nucleus-nucleus collisions. Throughout the paper, we restrict ourselves to collisions between nuclei of equal mass number.

II. THE MODEL

In this section, which is the central part of our paper, we present our model. In Sec. II A we describe how the primary nucleon distributions can be obtained from a multiple collision expansion of the Boltzmann equation. The connection with transport theory is established in Sec. II B, resulting in near-analytic expressions for the multiple collision components of the primary nucleon distributions.

The rescattering, or the final state interactions of the primordial nucleons, then leads to the final nucleon spectra as well as to the formation of composites. This is discussed in Sec. II C within the framework of the Hagedorn approach to the statistical thermodynamics of strong interactions. At the incident energies discussed in this paper, an appreciable amount of pions is produced. How we deal with pion production is described in the closing (Sec. II D).

A. Multiple collision expansion of the Boltzmann equation

Since the INC approach presents the most elaborate microscopic description available we will start there. The kinetic equation which forms more or less the basis of the cascade approach is the Boltzmann equation. Here, the one-particle distribution function $N(\mathbf{r},\mathbf{p},t)$ is calculated as determined by the well-known covariant equation (cf., e.g., Ref. 10):

$$\left[E\frac{\partial}{\partial t}+\mathbf{p}\cdot\nabla\right]N(\mathbf{r},\mathbf{p},t)=\int\int\int[N_i'N_j'W(p_i'p_j'\,|\,pp_j)-NN_jW(pp_j\,|\,p_i'p_j')]d\omega_i'd\omega_j'd\omega_j\ , \tag{2.1}$$

where

$$d\omega=\frac{d\mathbf{p}}{p_0},\quad p^\mu=(p_0,\mathbf{p})=(E/c,\mathbf{p})$$

and $\mathbf{r}$ represents the coordinate vector, $\mathbf{p}$ the momentum vector (p^μ the four-momentum), and t the time variable. The Boltzmann equation contains two parts, i.e., the drift term [left-hand side of (2.1)] and the collision term [right-hand side of (2.1)], and we abbreviate the equation as follows:

$$D(N)=C(N,N)\ . \tag{2.2}$$

The collision probability W is related to the elementary nucleon-nucleon cross section as follows:

$$d\sigma=\frac{1}{v_{ij}E_iE_j}\int\int W(p_ip_j\,|\,p_i'p_j')d\omega_i'd\omega_j'\ , \tag{2.3}$$

where v_{ij} is the relative velocity of the colliding particles and W still contains the conservation of total momentum and total energy

$$W(p_ip_j\,|\,p_i'p_j')=w(p_ip_j\,|\,p_i'p_j')\delta^{(4)}\times(p_i^\mu+p_j^\mu-p_i'^\mu-p_j'^\mu)\ . \tag{2.4}$$

The general relation between W and the differential cross section is then given as (valid in any reference system):

$$\frac{d\sigma}{d\Omega_{p_i'}}=\frac{1}{v_{ij}E_iE_j}\frac{(\mathbf{p}_i')^2}{E_iE_j}\left[\frac{dE_{\text{out}}}{d\,|\,\mathbf{p}_i'\,|}\right]^{-1}w(p_ip_j\,|\,p_i'p_j')\ , \tag{2.5}$$

$$E_{\text{out}}=E_{\text{out}}(\,|\,\mathbf{p}_i\,|\,,|\,\mathbf{p}_j\,|\,,|\,\mathbf{p}_i'\,|\,)\ ,$$

with E_{out} the total energy in the outgoing channel. For more details on the relativistic version of the Boltzmann equation we refer to the literature.[10]

In the energy region of interest, i.e., high bombarding energies, the nucleon-nucleon differential cross section is strongly forward-backward peaked. Since also initially the projectile and target nucleons are well separated in momentum space, we distinguish between beamlike (B) and targetlike (T) nucleons in the one-particle distribution function N:

$$N=N_B+N_T\ , \tag{2.6}$$

and

$$\begin{aligned}D(N_B)&=C(N_B,N_T)+C(N_B,N_B)\ ,\\ D(N_T)&=C(N_T,N_B)+C(N_T,N_T)\ ,\end{aligned} \tag{2.7}$$

which is equivalent to Eq. (2.2).

Our aim now is to simplify these equations assuming the nucleus-nucleus collision consists of two stages. First, there is the direct formation of a nonequilibrated region of participant nucleons. Second, in the expansion stage, the complicated dynamics of the formation, breakup, reformation, etc., of light fragments through final state interactions and rescattering between participants takes place. We recognize both stages in Eqs. (2.7). Since $C(N_B,N_B)$ and $C(N_T,N_T)$, respectively, describe gentle final state interactions among beamlike or targetlike participants while the remainder of the equations deals with the primary violent nonequilibrium "production" of beamlike or targetlike participants, we will now assume that both stages can be decoupled from each other. In other words, we neglect the effect of rescattering on the first stage which is then governed by the linearized coupled equations:

$$\begin{aligned}D(N_B)&=C(N_B,N_T)\ ,\\ D(N_T)&=C(N_T,N_B)\ .\end{aligned} \tag{2.8}$$

Rescattering will be an important mechanism towards the establishment of local equilibrium among beamlike or targetlike participants which, if it would be reached immediately, implies $C(N_B,N_B)=0$ and $C(N_T,N_T)=0$. Furthermore, it will give rise to composites (deuterons, tritons, etc.) as well, through final state interactions. Hence, we will impose, in an *a posteriori* fashion, local thermal and chemical equilibrium on the primary participants distribution [as obtained from (2.8)] as the major effect of rescattering. This will be discussed in more detail in Sec. II C.

The set of linearized equations (2.8) will now be rewritten in terms of a multiple collision series as follows. In

terms of a formal expansion parameter ϵ, which has to be taken as $\epsilon=1$ at the end, one can write

$$D(N_{B,T})=C_L(N_{B,T},N_{T,B})+\epsilon C_G(N_{B,T},N_{T,B}) ,$$
$$N_{B,T}=\sum_{n=0}^{\infty}\epsilon^n N_{B,T}^{(n)} , \tag{2.9}$$

and by substituting the last equation into the first and considering terms in ϵ^n, one obtains an iterative set of equations for $N_{B,T}^{(n)}$:

$$D(N_{B,T}^{(0)})=C_L(N_{B,T}^{(0)},N_{T,B}) ,$$
$$D(N_{B,T}^{(n)})=C_L(N_{B,T}^{(n)},N_{T,B})+C_G(N_{B,T}^{(n-1)},N_{T,B}),\quad n\geq 1 . \tag{2.10}$$

Note that we either expanded N_B or N_T depending on which of the equations (2.8) was considered. The terms C_L and C_G correspond to the loss and gain term (respectively, with minus and plus sign) in (2.1) and we have the formal equality $C(\ )=C_L(\ )+C_G(\ )$. The zeroth-order distribution functions $N_B^{(0)}$ and $N_T^{(0)}$ represent at $t\to-\infty$ the projectile—respectively, target spectator distributions which are given by the expression:

$$N^{(0)}(\mathbf{r},\mathbf{p},t\to-\infty)=\rho(\mathbf{r})f_F(\mathbf{p}) , \tag{2.11}$$

where $\rho(\mathbf{r})$ is the mass density for either projectile or target taken as a Woods-Saxon form normalized to the nuclear mass number and $f_F(\mathbf{p})$ is the Fermi momentum distribution which is taken as a Gaussian form with a width $2\sigma_F^2=\frac{2}{5}k_F^2$ (Fermi momentum $k_F=0.25$ GeV/c).

Equations (2.10) are still very cumbersome to solve mainly because they are coupled to each other. As is clear from Eq. (2.10), in $N_{B,T}^{(n)}$ each order of n is coupled to all orders $N_{T,B}^{(n)}$ since $N_{T,B}=\sum_n N_{T,B}^{(n)}$. On the other hand, if we view the collisions as proceeding sequentially, i.e., the average number of collisions $\bar{n}(t)$ as a function of time t increasing monotonically with t, then not all orders $N_{T,B}^{(n)}$ are equally important for $N_{B,T}^{(1)}$ or $N_{B,T}^{(\infty)}$, taking the two extremes. The first collision $n=1$ is dominated by the interaction of (cold) spectator beamlike particles with spectator targetlike particles, and therefore we can approximate the corresponding equation in Eq. (2.10) as follows:

$$D(N_B^{(1)})=C_L[N_B^{(1)},N_T^{(0)}(t=-\infty)]+C_G[N_B^{(0)}(t=-\infty),N_T^{(0)}(t=-\infty)] , \tag{2.12}$$

and similarly for $N_T^{(1)}$ with the $N^{(0)}$ distributions fixed at $t=-\infty$ and given by the expression (2.11). For the next collisions $n>1$, which will tend to equilibrate the system more and more, we take the other extreme, i.e.,

$$D(N_B^{(n)})=C_L[N_B^{(n)},N_T^{(\infty)}(t=+\infty)]+C_G[N_B^{(n-1)},N_T^{(\infty)}(t=+\infty)],\quad n>1 , \tag{2.13}$$

which describes the consecutive scatterings of beamlike or targetlike nucleons in an equilibrated stationary host medium $N_T^{(\infty)}(t=+\infty)$ which we assume to be of the form

$$N_T^{(\infty)}(\mathbf{r},\mathbf{p},t=+\infty)=\rho_T(\mathbf{r})f_E(\mathbf{p}) . \tag{2.14}$$

Here $f_E(\mathbf{p})$ is the equilibrium momentum distribution of the host medium (targetlike) which we take as a Maxwell-Boltzmann distribution with a temperature τ still to be determined. The most crude approximation involved is the use of the undisturbed mass density $\rho_T(\mathbf{r})$ in Eq. (2.14). Doing so, we assume that normal nuclear density is somehow to be expected on the average during the collision. This is in line with the use of the Boltzmann equation which is valid only for dilute systems. If complicated high density profiles occur during the collision process then this approximation definitely breaks down, but also the whole starting point of our approach is no longer valid. Otherwise, we expect it to be more or less reasonable.

The resulting set of equations for the multiple collision series expansion (2.9) is now given by Eq. (2.12) with Eq. (2.11), and Eq. (2.13) with Eq. (2.14), both of which have the same structural form. More explicitly one gets in the laboratory frame for either beamlike or targetlike participants:

$$\left[\frac{\partial}{\partial t}+\mathbf{v}\cdot\nabla\right]N^{(n)}(\mathbf{r},\mathbf{p},t)=-\sigma_{\text{tot}}\rho(\mathbf{r})vN^{(n)}(\mathbf{r},\mathbf{p},t)\int d\mathbf{p}'K_\alpha(\mathbf{p}'\mid\mathbf{p})+\sigma_{\text{tot}}\rho(\mathbf{r})\int d\mathbf{p}'v'K_\alpha(\mathbf{p}\mid\mathbf{p}')N^{(n-1)}(\mathbf{r},\mathbf{p}',t) , \tag{2.15}$$

where $v=|\mathbf{p}/E|$ and

$$K_\alpha(\mathbf{p}_4\mid\mathbf{p}_1)=\frac{1}{EE_1v_1}\int d\omega_2 d\omega_3\frac{1}{\sigma_{\text{tot}}}W(p_1p_2\mid p_3p_4)f_\alpha(\mathbf{p}_2) , \tag{2.16}$$

$\alpha=E,F$.

Here, $K_\alpha(\mathbf{p}\mid\mathbf{p}')$ is the scattering kernel which depends on $f_\alpha(\mathbf{p}_2)$, with $\alpha=F$ for the choice (2.11) at $n=1$ or $\alpha=E$ for the $n>1$ terms [Eq. (2.14)]. In both cases, to be discussed in Sec. II B, one has for $\alpha=E$ or $\alpha=F$ different expressions for $K_\alpha(\mathbf{p}\mid\mathbf{p}')$. The nucleon-nucleon total cross section σ_{tot} has been factorized out for convenience. Expressed in terms of the differential nucleon-nucleon cross section one finds from the relations (2.4) and (2.5):

$$K_\alpha(\mathbf{p}_4\mid\mathbf{p}_1)=\frac{1}{v_1}\int d\mathbf{p}_2v_{12}\delta(E_1+E_2-E_3-E_4)\left[\frac{dE_f}{dp_4}\right]\frac{1}{p_4^2}\left[\frac{1}{\sigma_{\text{tot}}}\frac{d\sigma}{d\Omega_4}\right]f_\alpha(\mathbf{p}_2) . \tag{2.17}$$

The quantity v_{12} is the relative velocity of particles 1 and 2. The partial differential equation (2.15) for $N^{(n)}(\mathbf{r},\mathbf{p},t)$ can be converted into an integral equation using the method of characteristics:

$$N^{(n)}(\mathbf{r},\mathbf{p},t)=\int_{-\infty}^{0} d\tau\sigma_{\rm tot}\rho(\mathbf{r}+\mathbf{v}\tau) \times\int d\mathbf{p}'K_\alpha(\mathbf{p}\mid\mathbf{p}')v'N^{(n-1)}(\mathbf{r}+\mathbf{v}\tau,\mathbf{p}',t+\tau)\exp\left[-\int_{\tau}^{0} d\tau' v\sigma_{\rm tot}\rho(\mathbf{r}+\mathbf{v}\tau')\int d\mathbf{p}'K_\alpha(\mathbf{p}'\mid\mathbf{p})\right] . \quad (2.18)$$

We now introduce the stationary distribution function $P^{(n)}(\mathbf{r},\mathbf{p})$ which counts at position $\mathbf{r}$ the total number of particles per unit of time within $d\mathbf{p}$, which have experienced n scatterings moving through a unit surface element perpendicular to $\mathbf{p}$ for all times:

$$P^{(n)}(\mathbf{r},\mathbf{p})\equiv|\mathbf{v}|\int_{-\infty}^{+\infty} dt\, N^{(n)}(\mathbf{r},\mathbf{p},t) , \quad (2.19)$$

where $\mathbf{v}$ is the velocity in the direction of $\mathbf{p}$. The definition (2.19) defines a flux of particles and can easily be related to a cross section. We then obtain from Eq. (2.18):

$$P^{(n)}(\mathbf{r},\mathbf{p})=\int_0^{\infty} d\eta\,\rho(\mathbf{r}-\eta)\sigma_{\rm tot}\int d\mathbf{p}'K_\alpha(\mathbf{p}\mid\mathbf{p}')P^{(n-1)}(\mathbf{r}-\eta,\mathbf{p}')\exp\left[-\int_0^{\eta} d\eta'\rho(\mathbf{r}-\eta')\sigma_{\rm tot}\int d\mathbf{p}'K_\alpha(\mathbf{p}'\mid\mathbf{p})\right] , \quad (2.20)$$

with $\alpha=F$ for $n=1$, $\alpha=E$ for $n>1$, where η is a vector along the $\mathbf{v}$ axis.

Equation (2.20) can be solved numerically as was done in Ref. 11, where average depleted mass distributions (of order n) were used instead of the undisturbed ones appearing in the equation here. However, this still remains a very complicated task and therefore we use an appropriate high-energy approximation known as the eikonal approximation. This means that we replace the zig-zag coordinate path of the nucleons by a straight line in the z direction, i.e., we replace η by $z\hat{\mathbf{z}}$ in Eq. (2.20). An immediate result is the fact that the distribution function $P^{(n)}(\mathbf{r},\mathbf{p})$ becomes separable in coordinate and momentum space

$$P^{(n)}(\mathbf{r},\mathbf{p})=G^{(n)}(\mathbf{r})M^{(n)}(\mathbf{p}) . \quad (2.21)$$

The functions $G^{(n)}$ and $M^{(n)}$ are governed by the equations (where $\hat{\mathbf{z}}$ denotes a unit vector in the z direction)

$$G^{(n)}(\mathbf{r})=\int_0^{\infty} dz''\rho(\mathbf{r}-z''\hat{\mathbf{z}})\sigma_{\rm tot}G^{(n-1)}(\mathbf{r}-z''\hat{\mathbf{z}}) \times\exp\left[-\int_0^{z''} dz'\rho(\mathbf{r}-z'\hat{\mathbf{z}})\sigma_{\rm tot}\right] ,$$

$$M^{(n)}(\mathbf{p})=\int d\mathbf{p}'K_\alpha(\mathbf{p}\mid\mathbf{p}')M^{(n-1)}(\mathbf{p}') , \quad (2.22)$$

which follow from Eq. (2.20) using the eikonal prescription and the assumption that $\sigma_{\rm tot}$ is independent of the bombarding energy which is reasonable at high energies. Also, replacing v_{12} by v_1 in (2.17) we find

$$\int d\mathbf{p}'K_\alpha(\mathbf{p}'\mid\mathbf{p})=1 . \quad (2.23)$$

The geometrical part $G^{(n)}(\mathbf{r})$ can be reduced to a familiar expression. Taking its asymptotic value $z\to+\infty$ corresponding to the scattering condition, one obtains from Eq. (2.22)

$$G^{(n)}(\mathbf{b},z=+\infty)=\frac{1}{n!}\left[\sigma_{\rm tot}\int\rho(\mathbf{b},z')dz'\right]^n \times\exp\left[-\sigma_{\rm tot}\int\rho(\mathbf{b},z')dz'\right] , \quad (2.24)$$

which are the well-known Glauber-Matthiae factors[12] for nucleon-nucleus scattering and where $\mathbf{b}$ denotes the impact parameter. For a nucleus-nucleus collision we have to fold in the initial projectile (the target) mass distribution $\rho_{\rm in}$:

$$G^{(n)}(\mathbf{b})=\int dz'd\mathbf{b}'\rho_{\rm in}(\mathbf{b}'-\mathbf{b},z') \times G^{(n)}(\mathbf{b}',z=+\infty) , \quad (2.25)$$

with $G^{(n)}(\mathbf{b},z=+\infty)$ given by the relation (2.24).

Equations (2.22), (2.24), and (2.25) are the key results on which we base our further study. They can be solved and from their solutions one can construct the primary participant distribution. If we would completely discard rescattering then one could calculate the nucleon inclusive cross section immediately from the expression (equal colliding nuclei):

$$\frac{d\sigma}{d\mathbf{p}}=A\sum_{n=1}^{\infty}\int d\mathbf{b}\,G^{(n)}(\mathbf{b})[M_B^{(n)}(\mathbf{p})+M_T^{(n)}(\mathbf{p})] , \quad (2.26)$$

with the nucleon mass number A, the Glauber-Matthiae geometrical factors $G^{(n)}(\mathbf{b})$, and the corresponding momentum distributions $M_B^{(n)}(\mathbf{p})$ and $M_T^{(n)}(\mathbf{p})$ of beamlike and targetlike nucleons normalized to unity. This has been done in Ref. 13.

In Sec. II C we will show how to modify Eq. (2.26) to take rescattering into account. First of all we will show how the basic equations (2.22) for $M^{(n)}(\mathbf{p})$ can be solved in a near-analytical way. Here we follow closely Ref. 14.

B. Connection with transport theory

The iteration equation (2.22) for $M^{(n)}(\mathbf{p})$, $n>1$ can be approximated by a Fokker-Planck equation, if the NN differential cross section has a smooth exponential dependence on the invariant momentum transfer squared t, i.e., if

$$\frac{d\sigma}{dt}=\left[\frac{d\sigma}{dt}\right]_{t=0}\exp(t/\Gamma^2) . \quad (2.27)$$

In this case, the right-hand side (rhs) of the iterative equation for $M^{(n)}(\mathbf{p})$ can be expanded to second order in $\boldsymbol{\zeta}=\mathbf{p}-\mathbf{p}'$. This leads to the Fokker-Planck equation

$$\frac{\partial}{\partial n}M^{(n)}(\mathbf{p})=\sum_{\lambda}\frac{\partial}{\partial p_\lambda}[C_\lambda M^{(n)}(\mathbf{p})] + \sum_{\lambda\mu}\frac{\partial^2}{\partial p_\lambda \partial p_\mu}[D_{\lambda\mu}M^{(n)}(\mathbf{p})],\quad n>1\ , \tag{2.28}$$

$$\lambda,\mu=1,2,3\ ,$$

where $D_{\lambda\mu}$ are the components of the diffusion tensor

$$D_{\lambda\mu}=\tfrac{1}{2}\langle\zeta_\lambda\zeta_\mu\rangle\ , \tag{2.29}$$

and C_λ are those of the drift vector

$$C_\lambda=-\left[\langle\zeta_\lambda\rangle+\sum_{\mu}\frac{\partial}{\partial p_\mu}D_{\lambda\mu}\right]. \tag{2.30}$$

We have used in Eqs. (2.29) and (2.30) the definitions

$$\begin{aligned}&\langle\zeta_\lambda\rangle\equiv\int d\boldsymbol{\zeta}\,\zeta_\lambda K_E(\mathbf{p}\mid\mathbf{p}')\ ,\\ &\langle\zeta_\lambda\zeta_\mu\rangle\equiv\int d\boldsymbol{\zeta}\,\zeta_\lambda\zeta_\mu K_E(\mathbf{p}\mid\mathbf{p}')\ ,\\ &\boldsymbol{\zeta}=\mathbf{p}-\mathbf{p}'\ .\end{aligned} \tag{2.31}$$

It is useful to consider Eqs. (2.28)—(2.31) in the nonrelativistic approximation. The collision kernel (2.17) can then, for the case $n>1$, be given in analytic form:

$$K_E(\mathbf{p}\mid\mathbf{p}')=\frac{1}{2\pi\Gamma^2}\frac{1}{\zeta}\exp(-\zeta^2/\Gamma^2) \times\exp(-p^2(\hat{\mathbf{p}}\cdot\hat{\boldsymbol{\zeta}})^2/2m\tau\ . \tag{2.32}$$

(Remember that for the case $n>1$ we use a Maxwell-Boltzmann distribution with temperature τ for the heat bath function f_E.)

For leading order of $p^2/2m\tau$ one then finds for the moments (2.31)

$$\langle\zeta_\lambda\rangle=-\beta p_\lambda,\quad\langle\zeta_\lambda^2\rangle=2D,\quad\langle\zeta_\lambda\zeta_\mu\rangle=0,\quad\lambda\neq\mu\ , \tag{2.33}$$

with

$$\beta\equiv\Gamma^2/(6m\tau),\quad D\equiv\tfrac{1}{6}\Gamma^2\ . \tag{2.34}$$

Equation (2.28) then takes the familiar form:

$$\frac{\partial}{\partial n}M^{(n)}(\mathbf{p})=(\beta\nabla_{\mathbf{p}}\cdot\mathbf{p}+D\Delta_p)M^{(n)}(\mathbf{p}) \tag{2.35}$$

describing the momentum distribution of a test nucleon moving in an equilibrated host medium with friction constant β and temperature τ. It follows from Eq. (2.34) that $m\tau\beta=D$, which is an analog to the Einstein relation known from Brownian motion. As a consequence, for an "infinitely" large number of collisions (in our case three or four) the thermal Maxwell distribution with temperature τ is reached.

In the relativistic regime, the kernel $K_E(\mathbf{p}\mid\mathbf{p}')$ (and hence its moments) cannot be evaluated analytically anymore. Therefore, the corresponding Fokker-Planck equation will be more complicated than Eq. (2.35). Nevertheless, we can obtain an approximate solution $M^{(n)}(\mathbf{p})$ by making use of the fact that the solution of Eq. (2.35) can be given in terms of a propagator G_n which is of Maxwellian form, and in terms of the distribution $M^{(1)}$ as initial condition. The relativistic generalization of this solution is given by[15]

$$M^{(n)}(\mathbf{p}^*)=\int\frac{d\mathbf{p}'^*}{E'^*}G_n(\mathbf{p}^*\mid\mathbf{p}'^*)M^{(1)}(\mathbf{p}^*\mid\mathbf{p}_0^*)\ , \tag{2.36}$$

where $\mathbf{p}_0^*$ is the incident momentum per nucleon. The asterisk denotes the fireball rest frame. We note that for identical nuclei (as we consider here) the fireball rest frame is equal to the c.m. frame of reference. The propagator G_n is given by

$$G_n(\mathbf{p}\mid\mathbf{p}')=N_nE\exp(-\{[m^2+(\mathbf{p}-\mathbf{p}'e^{-\beta(n-1)})^2]^{1/2}-m\}/\tau_n)\ , \tag{2.37}$$

with the normalization constant N_n:

$$N_n=(4\pi m^3)^{-1}\left[\frac{\tau_n}{m}\exp\left[\frac{m}{\tau_n}\right]K_2\left[\frac{m}{\tau_n}\right]\right]^{-1}, \tag{2.38}$$

where

$$\tau_n=\tau(1-e^{-2\beta(n-1)})\ . \tag{2.39}$$

The temperature τ of the heat bath (i.e., of the fireball) is determined by energy conservation

$$E_0^*=3\tau+m\frac{K_1\left[\frac{m}{\tau}\right]}{K_2\left[\frac{m}{\tau}\right]}\ , \tag{2.40}$$

where E_0^* is the incident energy per nucleon in the fireball frame and K_1,K_2 are the modified Bessel functions of first and second order, respectively. We note that for the friction constant β of Eqs. (2.37)—(2.39) we take over Eq. (2.34). Also, we assume the Einstein relation

$$m\tau\beta=D \tag{2.41}$$

to remain valid. The use of this relation is the reason that in Eqs. (2.37)—(2.39) only the friction constant β and the temperature τ of the heat bath appear, whereas the diffusion constant D is absent. With β fixed by Eq. (2.34) there is no free parameter left in our theory.

One can immediately verify from Eqs. (2.36) and (2.37) that

$$\begin{aligned}&\lim_{n\to1}M^{(n)}(\mathbf{p}^*)=M^{(1)}(\mathbf{p}^*)\ ,\\ &\lim_{n\to\infty}M^{(n)}(\mathbf{p}^*)=(4\pi m^3)^{-1}\left[\frac{\tau}{m}\exp\left[\frac{m}{\tau}\right]K_2\left[\frac{m}{\tau}\right]\right]\\ &\qquad\times e^{-E^*_{\mathrm{kin}}/\tau}\ .\end{aligned} \tag{2.42}$$

Hence, the function $M^{(n)}(\mathbf{p}^*)$, $n>1$ represents a smooth interpolation between the first collision and the thermal limit. The (nonstatistical) distribution function $M^{(1)}$ is

obtained by using the general scheme described in Sec. II B with the scattering kernel (2.16) involving the Fermi distribution f_F. To be more specific, $M^{(1)}$ is obtained from folding the Fermi distributions of the two colliding nucleons with the corresponding elementary cross section and integrating over all unobserved momenta. In general, this evaluation of $K(\mathbf{p}\,|\,\mathbf{p}')$ with a Fermi distribution $f_F(\mathbf{p})$ of Gaussian form with a width $2\sigma_F^2=\frac{2}{5}k_F^2$ (where k_F is the Fermi momentum), e.g., Eq. (2.17), has to be done numerically. But to a good approximation the result can be obtained analytically in the nonrelativistic approximation as

$$M_{B,T}^{(1)}(\mathbf{p}^*)=\frac{1}{\pi\Gamma^2}\left[\frac{2\sigma_F^2+\Gamma^2}{2\pi\sigma_F^2\Gamma^2}\right]^{1/2} e^{-(\mathbf{p}^*\mp\mathbf{p}_0^*)^2/\Gamma^2} \times e^{-(p^*-p_0^*)^2/2\sigma_F^2}. \tag{2.43}$$

More accurate expressions can be found in Ref. 16.

As we shall see in Sec. II C we finally only need the first and second moments of the function $M^{(1)}$. These can easily be generalized to the relativistic regime.

C. Statistical thermodynamics and rescattering: The Hagedorn approach

We now discuss an approximate way to treat the collisions among beamlike or targetlike nucleons which we have neglected in Eq. (2.7) to arrive at the linearized Eqs. (2.8). These collisions will further contribute to the attainment of local equilibrium among the primary participants as obtained from Eq. (2.8). Rescattering of participants will thus lead to thermalization but also give rise to the formation of composites or the production of new species like mesons. The latter of course can also be produced in the primary stage and we will show in Sec. II D, for the case of pions, how to deal with them. Composites, however, are most likely produced in the rescattering stage when the relative momenta of the participants are small.

It seems to be impossible to calculate explicitly all these processes (see, however, Ref. 17 where the production of deuterons is treated in a rigorous way), and therefore one uses statistical thermodynamics. Here, the original complicated interacting ensemble is replaced by a new collection of noninteracting particles in local thermal and chemical equilibrium, including now, as new species specifically, the results of the interactions that are like bound states. The complicated dynamics is shifted into the density of states or phase space.

The remarks made before would apply very well in a situation where the interacting system has attained global equilibrium (fully equilibrated). However, here we are in a regime which is far from this idealized equilibrated state, and one cannot simply abandon all the nonequilibrium features present in a nucleus-nucleus reaction. For instance, we would like to keep the concept of the multiple collision series since the order of scattering n is correlated to a time scale. Furthermore, the first collision $n=1$ is very different from $n=\infty$, and since both on the average occur at different times they should be treated separately.

A nice prescription which combines both the nonequilibrium features from the primary stage and the statistical thermodynamical treatment of the rescattering stage has been given by Hagedorn and Ranft (Refs. 8 and 9). We will apply it to our situation as follows. Consider our previous result Eq. (2.26) for the inclusive cross section of primary nucleons. Incorporating rescattering as outlined above, we obtain for the inclusive cross section for species i (nucleons, deuterons,...) the expression:

$$\frac{d\sigma_i}{d\mathbf{p}^*}=\sum_{n=1}^{\infty}\int d\mathbf{b}\left[\underset{\mathbf{p}\to\mathbf{p}^*}{L}(\lambda_B^{(n)})\frac{dN_i}{d\mathbf{p}}(T_B^{(n)},\mu_B^{(n)})+\underset{\mathbf{p}\to\mathbf{p}^*}{L}(\lambda_T^{(n)})\frac{dN_i}{d\mathbf{p}}(T_T^{(n)},\mu_T^{(n)})\right], \tag{2.44}$$

with the thermodynamical spectrum for species i

$$\frac{dN_i}{d\mathbf{p}}(T,\mu)=\frac{g_iV}{(2\pi)^3}\left\{\exp\left[\frac{(p^2+m_i^2)^{1/2}-\mu_i}{T}\right]\pm1\right\}^{-1}, \tag{2.45}$$

with statistical weight $g_i=(2S_i+1)(2I_i+1)$ with spin S_i and isospin I_i, temperature T, and chemical potential μ_i given by the relation

$$\mu_i=(A_i-Z_i)\mu_n+Z_i\mu_p+B_i \tag{2.46}$$

expressing chemical equilibrium. The particle of type i has (A_i-Z_i) neutrons and Z_i protons and a binding energy B_i. The quantities μ_n and μ_p are the chemical potentials for neutrons and protons, respectively. The quantity V denotes the volume of the interaction zone and is a parameter (freeze-out volume) in the model within reasonable limits. The symbol

$$\underset{\mathbf{p}\to\mathbf{p}^*}{L}(\lambda)$$

stands for the Lorentz transformation from the rest frame where we assumed local equilibrium to the moving frame (velocity λ), which for equal nuclei is the fireball frame.

Comparing the expression (2.44) with the original one, Eq. (2.26), we see that the momentum distributions $M_{B,T}^{(n)}$ have been replaced by others expressing local (i.e., dependent on B, T, and n), thermal (temperature T), and chemical (chemical potentials μ_n,μ_p) equilibrium in their rest frames. The unknowns λ, T, μ_n, and μ_p are determined as follows. For each n and either beamlike B or targetlike T participants we construct the first and second moments of $M_{B,T}^{(n)}(\mathbf{p}^*)$:

$$\langle\mathbf{p}^*\rangle_n^{B,T}=\int\frac{d\mathbf{p}^*}{E^*}\mathbf{p}^*M_{B,T}^{(n)}(\mathbf{p}^*) \tag{2.47}$$

and

$$\langle E^* \rangle_n^{B,T} = \int \frac{d\mathbf{p}^*}{E^*} E^* M_{B,T}^{(n)}(\mathbf{p}^*) , \tag{2.48}$$

corresponding to the average momentum and average energy per nucleon (after the first stage) in the fireball rest frame. These moments can be evaluated directly using the results for $M_{B,T}^{(n)}$ of the previous section. One finds

$$\langle \mathbf{p}^* \rangle_n^{B,T} = \pm \langle \mathbf{p}^* \rangle_1 e^{-\beta(n-1)} , \tag{2.49}$$

$$\langle E^* \rangle_n^{B,T} = 3\tau_n + m \frac{K_1\left[\frac{m}{\tau_n}\right]}{K_2\left[\frac{m}{\tau_n}\right]} + \langle E^*_{\rm kin} \rangle_1 e^{-2\beta(n-1)} . \tag{2.50}$$

Equation (2.49) is an exact result, and Eq. (2.50) holds to a very good approximation.

In $\langle \mathbf{p}^* \rangle_n^{B,T}$ and $\langle E^* \rangle_n^{B,T}$ for $n > 1$ to be completely determined we need in addition the average momentum $\langle \mathbf{p}^* \rangle_1^{B,T}$ and energy $\langle E^*_{\rm kin} \rangle_1^{B,T}$ after the first collision. Using the expression (2.43) for $M_{B,T}^{(1)}(\mathbf{p})$ we obtain

$$\langle \mathbf{p}^* \rangle_1^{B,T} = \left\{ 0,0,\pm p_0^* \left[1 - \frac{\Gamma^4}{2p_0^{*2}(2\sigma_F^2 + \Gamma^2)} \right] \right\} , \tag{2.51}$$

$$\langle E^*_{\rm kin} \rangle_1^{B,T} = (p_0^{*2} + m^2)^{1/2} - m + \frac{1}{2m} \frac{3}{2} \frac{2\sigma_F^2 \Gamma^2}{2\sigma_F^2 + \Gamma^2} , \tag{2.52}$$

where in the latter expression the nonrelativistic term $p_0^{*2}/2m$ has been replaced by its relativistic counterpart. It is worthwhile noting that Eq. (2.49) is valid in the nonrelativistic limit as well, whereas Eq. (2.50) becomes in this case

$$\langle E^* \rangle_n^{\rm NR} = \tfrac{3}{2}\tau_n + m + \langle E^*_{\rm kin} \rangle_1^{\rm NR} e^{-2\beta(n-1)} . \tag{2.53}$$

We shall use Eq. (2.50) in subsequent calculations.

Together with the known number of baryons and charges present we can now determine the variables λ, T, $\mu_{\rm n}$, and $\mu_{\rm p}$ appearing in Eq. (2.44). First of all we have for the velocity λ:

$$\lambda_{B,T}^{(n)} = \langle \mathbf{p}^* \rangle_n^{B,T} / [(\langle \mathbf{p}^* \rangle_n^{B,T})^2 + m^2]^{1/2} . \tag{2.54}$$

The total number n_i of particles of type i and the corresponding average energy ϵ_i can be constructed from the expression (2.45) as

$$n_i = \frac{g_i V m_i^2 T}{2\pi^2} \sum_{n=1}^{\infty} \frac{(\mp)^{n+1}}{n} \exp\left[\frac{n\mu_i}{T}\right] K_2\left[\frac{nm_i}{T}\right] , \tag{2.55}$$

$$\epsilon_i = \frac{g_i V m_i^3 T}{2\pi^2} \sum_{n=1}^{\infty} \frac{(\mp)^{n+1}}{n} \exp\left[\frac{n\mu_i}{T}\right] \times \left[K_1\left[\frac{nm_i}{T}\right] + \frac{3T}{nm_i} K_2\left[\frac{nm_i}{T}\right] \right] . \tag{2.56}$$

Then the conservation laws for total baryon number $\tilde{N}^{(n)}$, total charge number $\tilde{Z}^{(n)}$, and total energy $\tilde{\epsilon}^{(n)}$ in the participant zone enables one to obtain $\mu_{\rm n}$,$\mu_{\rm p}$ and T, for each n and each B or T subsystem separately:
T subsystem separately:

$$\tilde{N}_{B,T}^{(n)} = \sum_i A_i n_i ,$$
$$\tilde{Z}_{B,T}^{(n)} = \sum_i Z_i n_i , \tag{2.57}$$
$$\tilde{\epsilon}_{B,T}^{(n)} = \sum_i \epsilon_i ,$$

with

$$\tilde{\epsilon}_{B,T}^{(n)} \equiv \tilde{N}_{B,T}^{(n)} [\gamma_n^{B,T} (\langle E^* \rangle_n^{B,T} - \boldsymbol{\lambda}_{B,T}^{(n)} \langle \mathbf{p}^* \rangle_n^{B,T})]$$

and (2.58)

$$\gamma_n^{B,T} = [1 - (\boldsymbol{\lambda}^{(n)})_{B,T}^2]^{-1/2} .$$

The quantities $\tilde{N}_{B,T}^{(n)}$ and $\tilde{Z}_{B,T}^{(n)}$ are obtained from the number of participants calculated in the clean-cut participant-spectator geometry of Ref. 18.

D. Pion production

Beyond an incident energy of 0.6 GeV/nucleon pion production becomes an important aspect in nucleus-nucleus collisions and has to be treated properly. In our model pionic degrees of freedom enter in two ways according to the two stages envisioned in the dynamics of the reaction. Firstly, it is necessary to incorporate the direct production of pions in the first stage since about half of the total nucleon-nucleon cross section goes into inelastic (pion production) channels. Secondly, the rescattering between the primary nucleon participants will produce also pions for the same reason. In this second stage we treat the dynamics in a statistical way, and pions occur as one definite species i in the local thermal and chemical equilibrium of the total ensemble as described in Sec. II C.

One can easily modify the transport model of Sec. II B to take direct pion production into account.

Just as in the INC models we assume pion production to be mediated by the $\Delta(\frac{3}{2},\frac{3}{2})$ resonance through the inelastic reactions $\mathrm{N} + \mathrm{N} \rightarrow \mathrm{N} + \Delta$, and pion absorption by means of the inverse reaction $\mathrm{N} + \Delta \rightarrow \mathrm{N} + \mathrm{N}$. Taking the $\mathrm{N} + \mathrm{N} \rightarrow \mathrm{N} + \Delta$ differential cross section for Δ production to be the same as for the $\mathrm{N} + \mathrm{N} \rightarrow \mathrm{N} + \mathrm{N}$ channel, we obtain for the $n = 1$ (first collision) momentum distribution $M_\Delta^{(1)}(\mathbf{p}^*)$:

$$M_\Delta^{(1)}(\mathbf{p}^*) \propto e^{-(\mathbf{p}^* - \mathbf{p}_0)^2/\Gamma^2} e^{-(p^* - r^*)^2/2\sigma_F^2} , \tag{2.59}$$

where

$$(r^*)^2 = \tfrac{1}{4}s + (m_\Delta^2 - m^2)^2/4s - \tfrac{1}{2}(m_\Delta^2 + m^2) \tag{2.60}$$

and $m_\Delta = 1.235\ \mathrm{GeV}/c^2$ is the Δ mass, and s is the c.m. energy squared. The corresponding average momentum and kinetic energy of the Δ after the first collision then are

$$\langle p^* \rangle_1^\Delta = \frac{2\sigma_F^2 p_0^* + \Gamma^2 r^*}{2\sigma_F^2 + \Gamma^2} \left[1 - \frac{\Gamma^4 r^*}{2p_0^*} \frac{2\sigma_F^2 + \Gamma^2}{(2\sigma_F^2 p_0^* + \Gamma^2 r^*)^2} \right] \tag{2.61}$$

and

$$\langle E^* \rangle_1^{\Delta} = \frac{1}{2m_\Delta} \left[\left[\frac{2\sigma_F^2 \Gamma^2}{2\sigma_F^2 + \Gamma^2} \right]^2 \left[\frac{r^*}{2\sigma_F^2} + \frac{p_0^*}{\Gamma^2} \right]^2 + \frac{2}{3} \frac{2\sigma_F^2 \Gamma^2}{2\sigma_F^2 + \Gamma^2} \right] . \quad (2.62)$$

Although nonrelativistic, Eq. (2.62) turns out to be, because of the large Δ mass, a good enough approximation for our purposes. Also, we note the relation corresponding to Eq. (2.40) for the determination of the temperature τ in the presence of Δ resonances:

$$E_0^* = 3\tau + \rho_N m \frac{K_1\left[\frac{m}{\tau}\right]}{K_2\left[\frac{m}{\tau}\right]} + \rho_\Delta m_\Delta \frac{K_1\left[\frac{m_\Delta}{\tau}\right]}{K_2\left[\frac{m_\Delta}{\tau}\right]} , \quad (2.63)$$

where

$$\rho_N = \frac{4m^{3/2} e^{-m/\tau}}{4m^{3/2} e^{-m/\tau} + 16 m_\Delta^{3/2} e^{-m_\Delta/\tau}} , \quad (2.64)$$

$$\rho_\Delta = \frac{16m^{3/2} e^{-m_\Delta/\tau}}{4m^{3/2} e^{-m/\tau} + 16 m_\Delta^{3/2} e^{-m_\Delta/\tau}} , \quad (2.65)$$

$$\rho_N + \rho_\Delta = 1 . \quad (2.66)$$

Now we have to find out how many of the initial nucleons are converted into Δ resonances after the first collision. This number is fixed by the branching ratio α for either the $N + N \to N + N$ or $N + N \to N + \Delta$ channel to occur. Assuming the spin-averaged transition probability for the elastic process $N + N \to N + N$ to be given by $|t_{el}|^2$, and the inelastic spin-averaged transition probability given by $|t_{inel}|^2$, we have

$$\alpha = \frac{|t_{inel}|^2}{|t_{el}|^2 + |t_{inel}|^2} = \frac{\sigma_{NN\to N\Delta}}{2\sigma_{NN\to NN} + \sigma_{NN\to N\Delta}} . \quad (2.67)$$

Taking now

$$\sigma_{tot} = \sigma_{NN\to NN} + \sigma_{NN\to N\Delta} = 42 \text{ mb} ,$$

all we need is an estimate for $\sigma_{NN\to N\Delta}$. For this cross section we take the pion production cross section $N + N \to N + N + \pi$ as calculated by Bertsch.[19] This author has calculated the effective pion production cross section, modified for the scattering of nucleons from two Fermi spheres and respecting the Pauli exclusion principle. The values obtained in this way for the branching ratio α are listed in Table I and are different, especially at low bombarding energies, from the ones obtained by using the free (measured) pion production cross section instead of the effective one.

Except for the very high bombarding energies (2.1 GeV/nucleon) it seems reasonable to include the Δ dynamics only in the first collision ($n = 1$) contribution to the primary participants distribution (first stage). In this way only creation of deltas has to be considered, since for absorption one needs at least one additional collision. In subsequent collisions ($n > 1$) the average available energy is degraded so much that either the inelastic channel is closed or pion production mechanisms other than through the isobar mechanism are important. They will however contribute very little as compared to the first collision. Therefore we disregard Δ dynamics completely in the primary, first stage for all $n > 1$.

Another source of pions originates from the rescattering between beamlike or projectilelike participants. Pionic degrees of freedom can be included easily in the statistical thermodynamics by regarding the pions or deltas specifically as a species to be included in the formalism of Sec. II C. For $n = 1$ we have, before rescattering, a mixture of nucleons and delta resonances for which we know the relative abundance, and the average momenta and average energies separately. From these quantities we construct the average velocity of the combined system and the corresponding average energy available in this mixed ensemble of nucleons and deltas. These then serve as input for our thermodynamical treatment of rescattering equations (2.57) and (2.58). The effect of rescattering in the initial collection of nucleons and deltas in $n = 1$ is thermodynamically expressed in the establishment of local thermal and chemical equilibrium in a collection of different species $\{i\}$, where we include both deltas and pions besides nucleons and composites. Thus rescattering or final state interactions convert the original deltas into deltas

TABLE I. Input data for the calculation of the final inclusive particle cross sections.

E_0^{lab} (MeV)	τ (MeV)	β	$\langle \mathbf{p}^* \rangle_1$ (MeV/c)	$\langle E^* \rangle_1$ (MeV)	$\langle \mathbf{p}^* \rangle_1^{\Delta}$ (MeV/c)	$\langle E^* \rangle_1^{\Delta}$ (MeV)	α
400	59	$\frac{1}{2}$[a]	220[b]	95			
800	85	$\frac{1}{2}$	440	200	148	52	0.22
2100	160	$\frac{1}{5}$	900	446	755	300	0.35

[a]At these low energies the NN elementary cross sections are nearly isotropic and therefore the expression for β is not valid anymore. However, since in this energy regime $n_{relaxation} \simeq 3$ collisions are sufficient for equilibration and $\beta^{-1} \simeq n_{rel} - 1$, we can calculate β.

[b]These values are obtained by letting $\Gamma^2 \to \infty$ and replacing the Fermi distributions by δ functions, which leads to $\langle \mathbf{p}^* \rangle_1 = p_0^*/2$.

and pions (plus nucleons). By taking the number of deltas and pions after rescattering equal to the original number of deltas determined by the branching ratio α, one introduces a new constraint to be added to the ones already present in Eq. (2.57). This allows for calculating the chemical potentials μ_Δ and $\mu_\pi=\mu_\Delta-\mu_N$ where the latter is a consequence of the condition of chemical equilibrium. The remaining deltas after rescattering are now allowed to decay into nucleons and pions via $\Delta\rightarrow\pi+N$. The decay of the Δ is incorporated using explicit formulas given by Hagedorn and Ranft,[8,9] and taking into account the width of the Δ resonance $\Gamma_\Delta=112$ MeV/c^2 through an integration over an appropriate Lorentz form for the mass distribution. The resulting momentum spectrum in the rest frame where we assumed local equilibrium for particle i (either pion or nucleon) resulting from the two-body decay $m_\Delta\rightarrow m_i+m_j$ is then given by the expression:

$$\frac{dN_i}{d\mathbf{p}}=\frac{1}{2}\frac{g_i g_\Delta V}{(2\pi)^3}\int dm'_\Delta\rho(m_\Delta,m'_\Delta)\frac{T^2}{Epp_i}m'_\Delta \times\left[\left(1+\frac{\epsilon_-}{T}\right)e^{-\epsilon_-/T}-\left(1+\frac{\epsilon_+}{T}\right)e^{-\epsilon_+/T}\right]\times\frac{\mu_\Delta}{e^T}\,, \tag{2.68}$$

where

$$\epsilon_\pm=\frac{m'_\Delta}{m_i^2}(EE_i\pm pp_i)\,,$$
$$E_i=\frac{1}{2m'_\Delta}(m'^2_\Delta+m_i^2-m_j^2)\,,$$
$$p_i=\frac{1}{2m'_\Delta}\{[m'^2_\Delta-(m_i+m_j)^2][m'^2_\Delta-(m_i-m_j)^2]\}^{1/2}\,, \tag{2.69}$$
$$\rho(m_\Delta,m'_\Delta)=\frac{\Gamma_\Delta/2\pi}{(m_\Delta-m'_\Delta)^2+\Gamma_\Delta^2/4}\,,$$
$$m_\Delta=1235\ \text{MeV}/c^2,\quad \Gamma_\Delta=112\ \text{MeV}/c^2\,.$$

As we already mentioned there are no pionic degrees (or delta resonances) involved in the $n>1$ contributions to the primary participants distribution. The rescattering modification for $n>1$ will however include pions besides nucleons and composites. Therefore, for $n>1$ pions are produced thermally according to available energy with chemical potential $\mu_\pi=0$.

To conclude this section we list in Table I the input used in our calculations at the various incident energies per nucleon and for equal nuclei.

III. NUMERICAL RESULTS AND COMPARISON WITH EXPERIMENT

The purpose of this section is twofold. Firstly, we want to emphasize those features of our model which distinguish it from thermal models and make it, despite its simplicity, similar in many respects to the much more complex nuclear cascade approaches. This is discussed in Sec. III A. Secondly, we wish to test our model for a wide range of incident energies and projectile-target masses by a comparison with appropriate experimental data. To keep the comparison transparent we mainly discuss gross features rather than details of all kinds of different production cross sections. For such details, we refer to our previous publications.[20–23] In Sec. III B we discuss the slopes of the nucleon and pion spectra as a function of the incident energy per nucleon. Beam energy and mass dependence of the composite particles to proton ratio are the subject of Sec. III C, as well as the beam energy dependence of the negative pion to the total nuclear charge ratio. The final Sec. III D is devoted to a comparison of our calculations for the proton and pion spectra with the corresponding experimental results at the incident energy of 2.1 GeV per nucleon. Throughout our calculations we take for the freeze-out volume V which enters as a parameter, a value such that the corresponding freeze-out density corresponds to half-normal nuclear matter density.

A. The role of the first collision and comparison with cascade calculations

The first collision contribution is instrumental for the agreement with the measured nucleon inclusive spectra at forward angles. This is illustrated clearly in Fig. 1 for the reaction Ar + KCl$\rightarrow$p + X at 800 MeV/nucleon, with data points taken from Ref. 7 but now displayed in a nonstandard fashion (log versus log plot). This figure shows that the quasifree peak of the primary first collision component prevails after taking rescattering through the Hagedorn prescription into account: The nonzero relative velocity between the center of mass frame (i.e., the fireball rest frame) and the first collision rest frame results in a shift of the fireball spectrum towards the experimentally observed one. The shift becomes less pronounced with growing outgoing laboratory angle and will finally disappear at large angles.

Figure 2 shows a comparison of the proton and pion inclusive spectra from our model with corresponding intranuclear cascade calculations[24] and with data from Ref. 7. In Fig. 2(a) the proton inclusive spectra from the Ar + KCl collision at 800 MeV/nucleon are displayed. Although some discrepancies remain at forward angles, the overall agreement of all calculations with each other and with the data is good. Corresponding pion spectra are shown in Fig. 2(b). Here, a comparison is made in addition with the intranuclear cascade calculations of Ref. 25. The latter calculation uses a scenario for pion production which is essentially the same as ours: Pions are created already *during* the collision and not only, like in Ref. 24, via the decay of stable delta resonances at the end of the collision.[26] Therefore, it is not surprising that our results are in better agreement with those of Ref. 25 than with those of Ref. 24. A common feature of the model calculations shown in Fig. 2(b) is that they overestimate, like almost all other models, the pion production rate. Possible explanations for this are given in Refs. 4, 21, and 27.

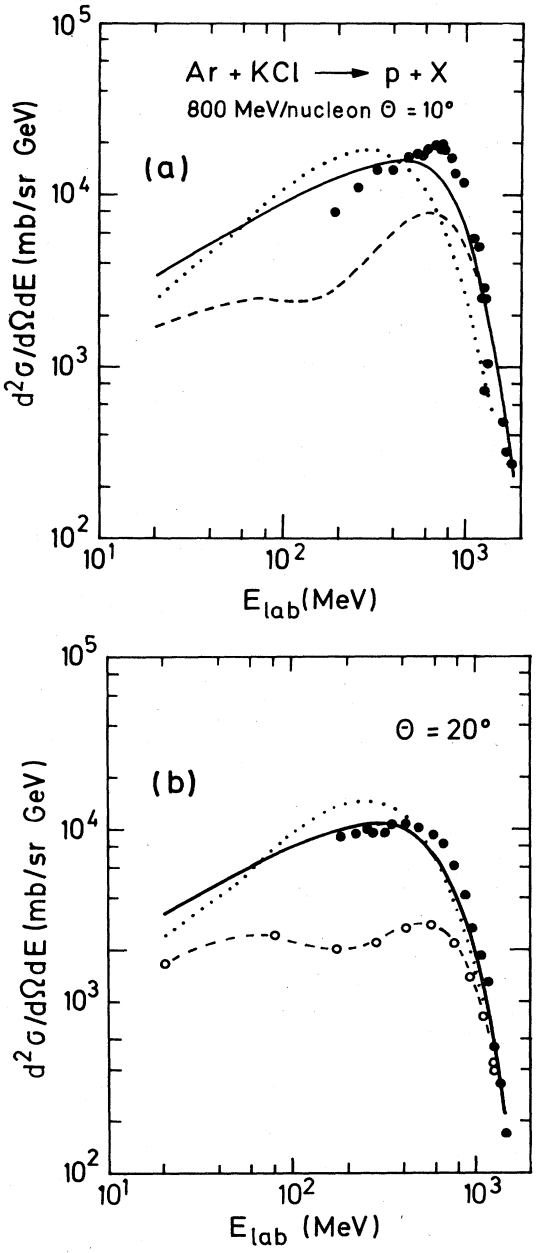

FIG. 1. The proton inclusive double differential cross section for the reaction 800 MeV/nucleon Ar + KCl as a function of the proton kinetic energy in the laboratory system. (a) For a laboratory angle of 10 deg. (b) For a laboratory angle of 20 deg. Full line: Our model. Dashed line: The quasifree component only. Dotted line: The fireball model (Ref. 36). Black circles: Experimental data of Ref. 7.

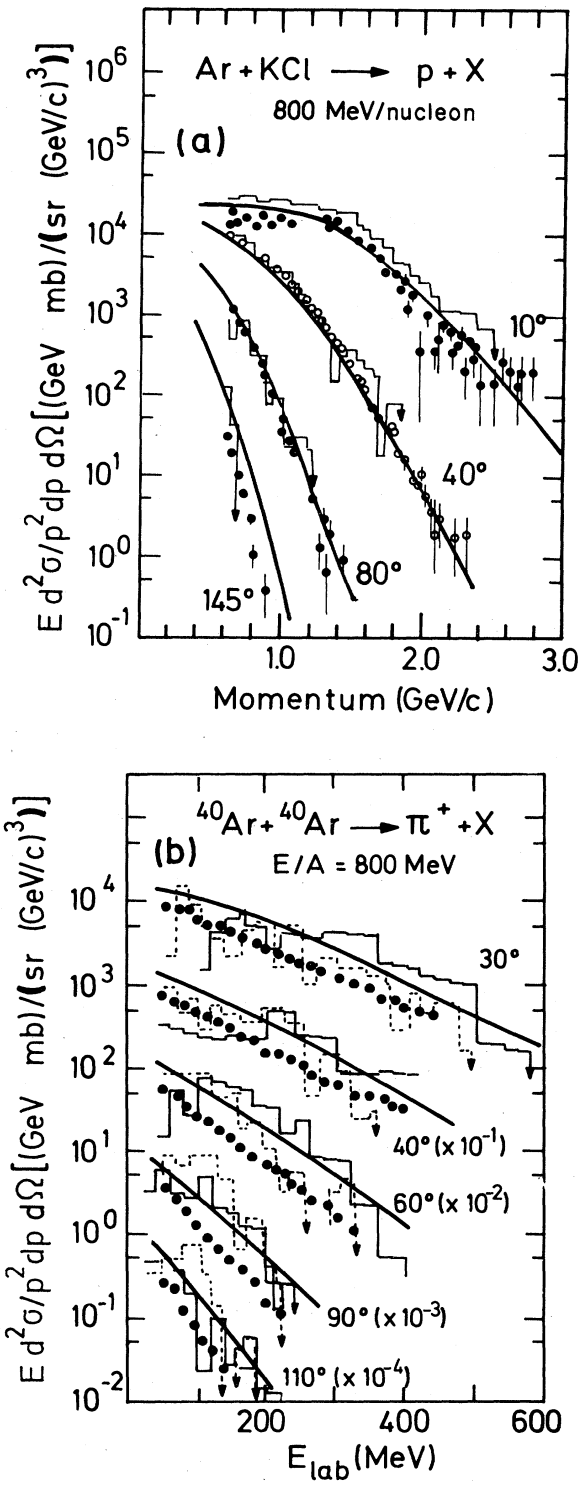

FIG. 2. The hadron inclusive invariant differential cross section for the reaction 800 MeV/nucleon Ar + KCl as a function of the hadron momentum in the laboratory system. Full lines: Our model. Histogram: The cascade model of Ref. 24. Full and open circles: Experimental data of Ref. 7. (a) For proton production. (b) For positive pion production. The dotted histogram denotes cascade model results of Ref. 25.

B. Exponential slope factors for high energy protons and pions as a function of the incident energy per nucleon

Nagamiya and collaborators observed that their measured proton and pion inclusive spectra at a c.m. angle of 90° could, apart from small deviations at low outgoing proton energies, be parametrized rather well by

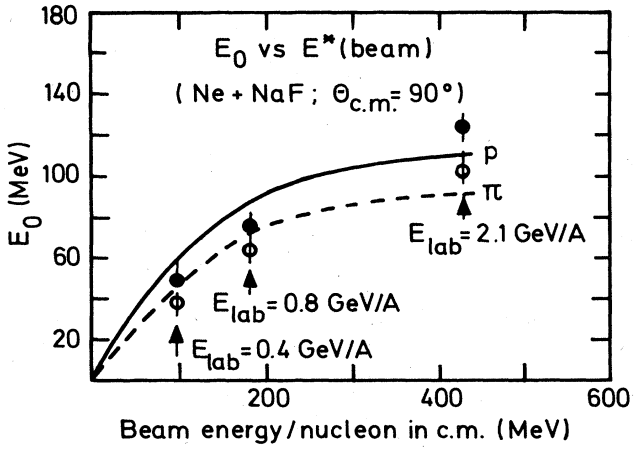

FIG. 3. The slope factor E_0 of the parametrized hadron inclusive cross section Eq. (3.1) as a function of the bombarding energy/nucleon in the c.m. system. The reaction considered is Ne + NaF at a c.m. angle of 90 deg. Full and dashed lines: Our model for proton and pion production, respectively. Full and open circles: Experimental data of Ref. 7 for proton and pion production, respectively.

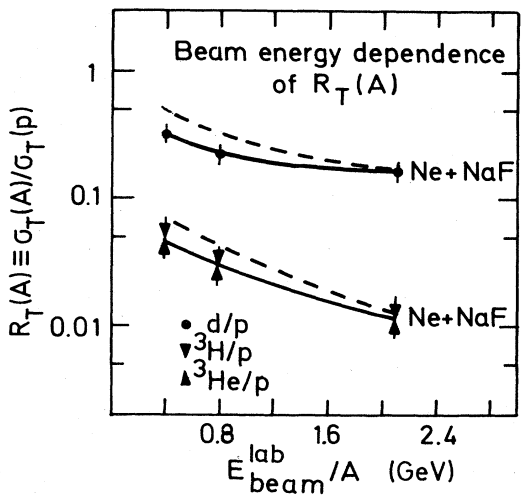

FIG. 4. The ratios of the d, ^{3}H, and ^{3}He inclusive total production cross sections to the proton inclusive total production cross section as a function of the bombarding energy per nucleon in the laboratory. The reaction considered is Ne + NaF. Dashed line: Our model. Circles and triangles: Experimental data of Ref. 7. The full line serves as a guide through the experimental points.

$$E\frac{d^3\sigma}{d^3p}\exp(-E_k^*/E_0)\ , \tag{3.1}$$

where E_k^* is the kinetic energy of the outgoing proton (pion).[28] The slope factor E_0 which is a measure for how much the participant region is heated up at the time of the particle emission and is sometimes called "apparent temperature," was then plotted at various beam energies/nucleon. We have done a similar analysis. The results are shown in Fig. 3 for the system Ne + NaF. The calculated slope factors are slightly too high at 400 and 800 MeV/nucleon and slightly too low at 2.1 GeV/nucleon. They are, like those extracted from the experimental data, different for protons and pions. This latter feature was some time ago, widely discussed in the literature (cf., e.g., Ref. 29). In our model, the reason for the lower apparent temperature of the pions as compared to that of the protons is twofold. Firstly, the transformation of the spectra from their local rest frame to the nucleus-nucleus c.m. frame lets the pions, because of their lighter mass, appear cooler than the protons. This explanation is formally similar to, but physically different from, the one given in Ref. 29. In the blast wave model of Ref. 29, the nonzero boost velocity is due to the collective flow in the expansion phase, whereas in our model it originates from the nonequilibrated component in the early phase of the collision. Secondly, the Δ-decay kinematics leads to a slope of the pion spectra steeper than that of the proton spectra.[13]

C. Ratios of composites to protons and of pions to the total nuclear charge

The beam energy dependence of d/p and ^{3}H(^{3}He)/p ratios is shown in Fig. 4. The collision is again Ne + NaF. It is seen that our model nicely reproduces the trend of the experimental data, although the ratios are somewhat too high at 400 MeV/nucleon. The d/p ratio has been related to entropy in Ref. 30 in a simple way by using the Sackur-Tetrode formula. Given that such a connection is meaningful in the case of heavy ion collisions we then obtain a satisfactory agreement with the calculated and measured entropy. This is in contrast to the results of Refs. 30 and 31, but in these works only central collisions were discussed. If in cascade calculations impact parameter averaging is performed the discrepancies essentially disappear.[32]

The mass dependences of the same ratios are displayed in Fig. 5 for a beam energy of 800 MeV/nucleon and the systems C + C, Ne + NaF, and Ar + KCl. Here we are in qualitative disagreement with the experimental data: The calculated ratios are essentially mass number independent, whereas the measured ratios grow larger with increasing masses. This disagreement persists for heavier systems as we have checked for the reaction ^{139}La + ^{139}La.

The ratio of negative pions to the total nuclear charge is shown in Fig. 6. At 400 and 800 MeV per nucleon, the agreement with the measured ratio is quite good, whereas at 2.1 GeV/nucleon our calculation yields too few pions. This could be due to the fact that there we neglected resonances with masses larger than that of the Δ whose decay also leads to pions.

D. Proton and pion inclusive spectra at 2.1 GeV/nucleon

The inclusive spectra at 2.1 GeV/nucleon are particularly interesting because our model makes a definite prediction here: It predicts a large transparency of the reaction because the number of collisions needed for equilibra-

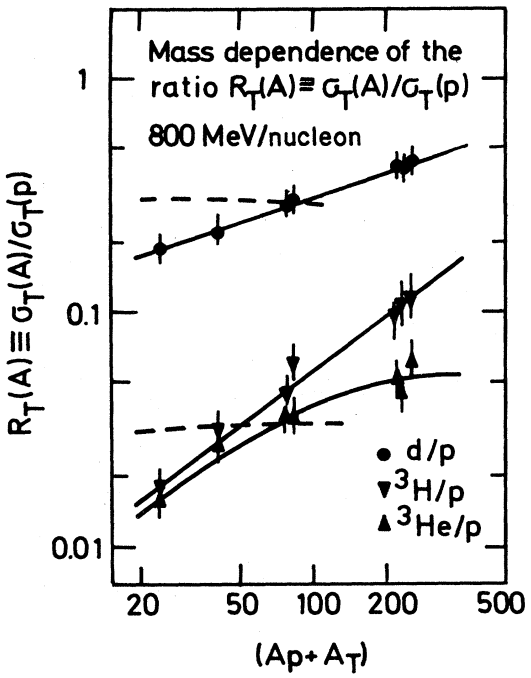

FIG. 5. The dependence of the ratios considered in Fig. 4 on the total mass number, at a fixed bombarding energy of 800 MeV/nucleon in the laboratory. See Fig. 4 for an explanation of the curves and symbols.

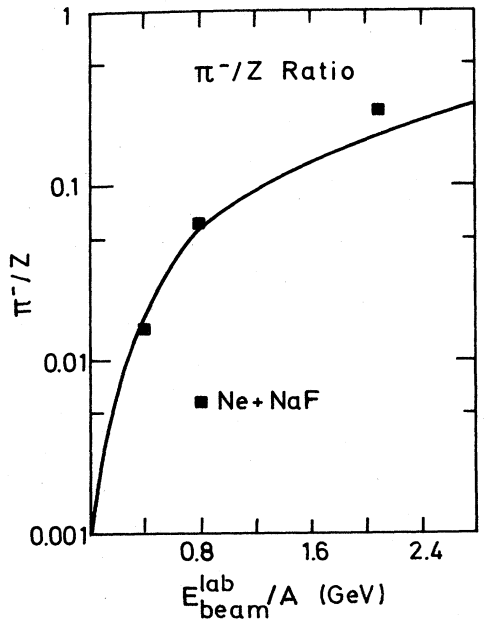

FIG. 6. The ratio of the number of negative pions to the total nuclear charge as a function of the bombarding energy/nucleon in the laboratory. The reaction is Ne + NaF. Full line: Our model. Squares: Experimental data of Ref. 7.

tion is approximately six to seven. This is due to the very strongly forward peaked elementary NN cross section which in turn results in a small friction constant (cf. Table I). How do our model calculations compare with the experimental data? In Fig. 7 such a comparison is done for the proton spectra with data from Ref. 33. The drawn line is the result of our model as it is discussed in Sec. II. The agreement with the data is overall satisfactory, the largest deviations being a factor of 2. The agreement could probably be improved if the input average momenta for treating the expansion stage would be treated separately for N's and Δ's as has been done in Ref. 34, where, however, composite particle and pion production has been neglected. In the c.m. system, our spectra are strongly anisotropic, in qualitative agreement with the experimental results of Ref. 7. Hence, the large percentage of nonequilibrated contributions to the inclusive proton spectrum is supported by experiment. The dashed line denotes the results of a scenario where the Δ is treated as a stable particle decaying into N and π only at the end of the heavy ion reaction and where composite particle production has been turned off. Apart at low momenta the proton spectrum is not very sensitive to the different scenarios.

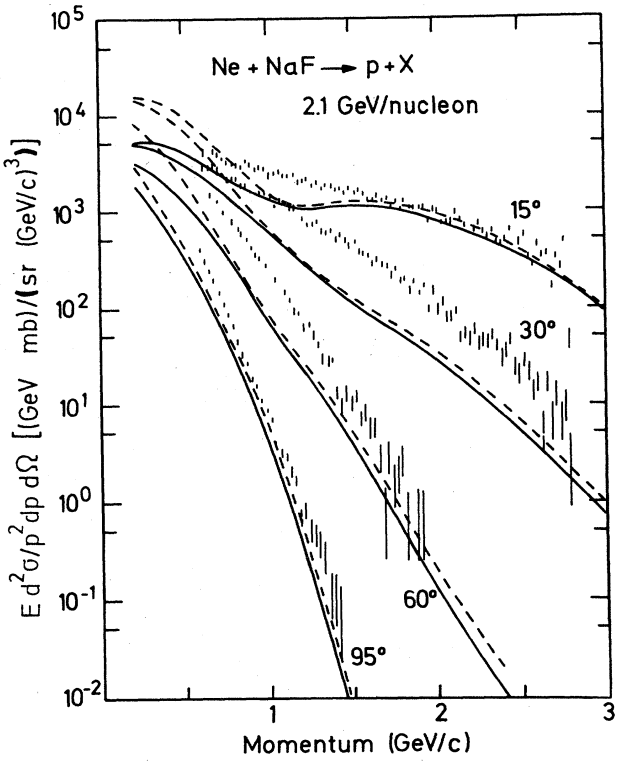

FIG. 7. The proton inclusive invariant differential cross section for the reaction Ne + NaF at 2.1 GeV/nucleon as a function of the proton laboratory momentum. Full lines: Our model. Dashed lines: Our model, but with pion production exclusively from stable delta resonances which are allowed to decay into a nucleon and a pion only at the end of the collision. The experimental data are from Ref. 33.

In Fig. 8, we show corresponding results for pion production. The agreement with the experimental points is seen to be very good. In contrast to the proton spectra, the pion spectrum is very sensitive to the production mechanism of the pions. In particular, the creation of pions *during* the reaction is seen to be vital; the spectra calculated with the assumption of stable Δ's is much worse compared to the data: The slopes are much too steep. This is consistent with previous calculations at 800 MeV/nucleon.[13]

IV. SUMMARY AND OUTLOOK

We have developed a simple multiple collision (transport) model which describes nucleon and meson as well as light fragment emission in the energy range of 400—2100 MeV per nucleon. Our approach is based on the relativistic Boltzmann equation. Through an expansion of the one-particle distribution function in terms of the number n of independent nucleon-nucleon (NN) collisions the Boltzmann equation is recast in an infinite set of coupled integro-differential equations. Linearizing these equations by neglecting the interactions of the test nucleons with each other and letting them scatter with partner nucleons whose distributions are stationary (Fermi distributions for the first collision $n=1$, thermal distributions for $n \geq 2$), they can be solved in the eikonal approximation. Each solution represents a multiple collision term with collision number n and factorizes in a coordinate dependent (geometrical) and a momentum dependent (dynamical) part. The geometrical part is given by the well-known Glauber-Matthiae factors, and the dynamical part is to a good approximation given by the solution of a Fokker-Planck—type equation with parameter-free drift and diffusion coefficients. These primary distribution functions are modified by final state interactions which we assume to lead to light fragment formation in the expansion phase of the collision. To obtain the final light fragment cross sections we use Hagedorn's thermodynamics of strong interactions for each multiple collision component in the corresponding local rest frame. At incident energies of 400 and 800 MeV per nucleon these local rest frames turn out to be appreciably different from the fireball rest frame only for the first collision, i.e., at these energies the main nonequilibrium features of the spectra arise from the quasifree component of the primary distribution. The situation is different at 2.1 GeV per nucleon. Here, according to our theory, the initial participant zone is highly nonequilibrated because of the small friction constant $\beta \simeq \frac{1}{5}$ (i.e., $\simeq 6$ collisions per nucleon are needed for equilibration). One therefore has to keep track also of the local fireballs for $n > 1$. Our results are not very sensitive to the parameter of the model which is the nuclear freeze-out volume as long as we choose it within reasonable limits.

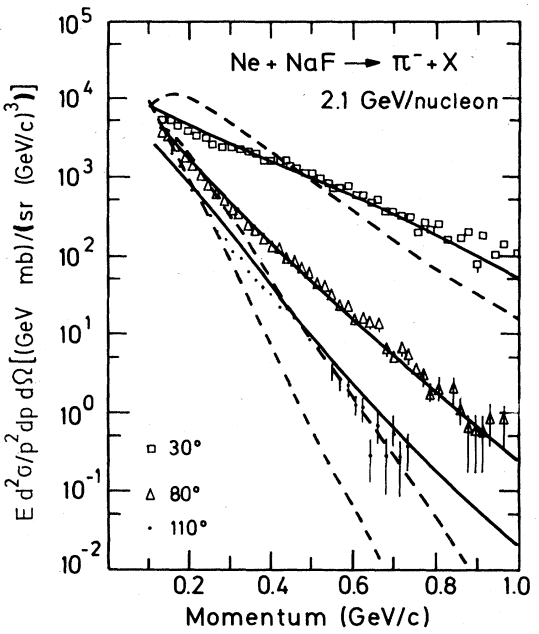

FIG. 8. Same as Fig. 7, except that in this figure pion production is considered.

To summarize, the agreement of our theory with the measured nucleon, pion, and light fragment inclusive spectra over a wide energy range of 400 MeV to 2.1 GeV per nucleon is overall satisfactory. Taking this together with the successful application of the model to strange meson production[34,35] we conclude that the transport theory for particle inclusive production provides a useful, simple, and transparent description of the corresponding experimental results.

We appreciate valuable discussions with S. Mies and W. Zwermann.

[1]For a review, see, i.e., S. Nagamiya and M. Gyulassy, Adv. Nucl. Phys. **13**, 201 (1984).

[2]For a review, see J. Cugnon, Nucl. Phys. **A387**, 191c (1982).

[3]A nice outline is given by G. E. Uhlenbeck, in *Lectures in Statistical Mechanics,* edited by G. E. Uhlenbeck and G. W. Ford (American Mathematical Society, Providence, RI, 1963). Its covariant formulation is discussed in Ref. 10 where further references can be found.

[4]R. Stock, R. Bock, R. Brockman, J. W. Harris, A. Sandoval, H. Stroebele, K. L. Wolf, H. G. Pugh, L. S. Schroeder, M. Maier, R. E. Renfordt, A. Dacal, and M. E. Ortiz, Phys. Rev. Lett. **49**, 1236 (1982).

[5]H. A. Gustafsson, H. H. Gutbrod, B. Kolb, H. Löhner, B. Ludewigt, A. M. Poskanzer, T. Renner, H. Riedesel, H. G. Ritter, A. Warwick, F. Weik, and H. Wieman, Phys. Rev. Lett. **52**, 1590 (1984).

[6]R. Malfliet, Nucl. Phys. **A420**, 621 (1984); Phys. Rev. Lett. **53**, 2386 (1984).

[7]S. Nagamiya, M. C. Lemaire, E. Moeller, S. Schnetzer, G. Shapiro, H. Steiner, and I. Tanihata, Phys. Rev. C **24**, 971

(1981).
[8]R. Hagedorn and J. Ranft, Nuovo Cimento Suppl. **6**, 169 (1968).
[9]R. Hagedorn, Nucl. Phys. **B24**, 93 (1970).
[10]R. Malfliet, Nucl. Phys. **A363**, 429 (1981), where further references can also be found.
[11]R. Malfliet, Phys. Rev. Lett. **44**, 864 (1980); Nucl. Phys. **A363**, 456 (1981).
[12]R. J. Glauber and G. Matthiae, Nucl. Phys. **B21**, 135 (1970).
[13]H. J. Pirner and B. Schürmann, Nucl. Phys. **A316**, 461 (1979); B. Schürmann, Phys. Rev. C **20**, 1607 (1979); M. Chemtob and B. Schürmann, Nucl. Phys. **A336**, 508 (1980).
[14]B. Schürmann and D. P. Min, Nucl. Phys. **A370**, 496 (1981).
[15]B. Schürmann, K. M. Hartmann, and H. J. Pirner, Nucl. Phys. **A360**, 435 (1981).
[16]W. Zwermann, Technical University of Munich Report TUM-TPhT30-118, 1984.
[17]M. Gyulassy, K. Frankel, and E. A. Remler, Nucl. Phys. **A402**, 596 (1983).
[18]J. Gosset, J. I. Kapusta, and G. D. Westfall, Phys. Rev. C **18**, 844 (1978).
[19]G. F. Bertsch, Phys. Rev. C **15**, 713 (1977).
[20]R. Malfliet, E. Martschew, and B. Schürmann, Phys. Lett. **124B**, 152 (1983).
[21]R. Malfliet and B. Schürmann, Phys. Rev. C **28**, 1136 (1983).
[22]B. Schürmann, in Proceedings of the International Conference on High Energy Nuclear Physics, Balatonfüred, Hungary, 1983, p. 469.
[23]R. Malfliet, see Ref. 22, p. 481.
[24]J. Cugnon, Phys. Rev. C **22**, 1885 (1980).
[25]Y. Yariv and Z. Fraenkel, Phys. Rev. C **20**, 2227 (1979).
[26]The cascade model (Ref. 24) has been improved by J. Cugnon, D. Kinet, and J. Vandermeulen, Nucl. Phys. **A379**, 557 (1982), to allow for pion production during the collision.
[27]M. Cahay, J. Cugnon, and J. Vandermeulen, Nucl. Phys. **A411**, 524 (1983).
[28]The c.m. angle of 90° is chosen to minimize the contributions from spectator particles and of the quasifree component.
[29]P. J. Siemens and J. O. Rasmussen, Phys. Rev. Lett. **42**, 880 (1979).
[30]P. J. Siemens and J. Kapusta, Phys. Rev. Lett. **43**, 1486 (1979).
[31]G. F. Bertsch and J. Gugnon, Phys. Rev. C **24**, 2514 (1981).
[32]G. F. Bertsch, Nucl. Phys. **A400**, 221c (1983).
[33]I. Tanihata *et al.*, Bevalac experiment No. E471H.
[34]W. Zwermann and B. Schürmann, Nucl. Phys. **A423**, 525 (1984).
[35]W. Zwermann and B. Schürmann, Phys. Lett. **145B**, 315 (1984).
[36]J. Gosset, H. H. Gutbrod, W. G. Meyer, A. M. Poskanzer, A. Sandoval, R. Stock, and G. D. Westfall, Phys. Rev. C **16**, 629 (1977).